TECHNISCHE MECHANIK, 30, 1-3, (2010), 185 - 194
submitted: October 31, 2009

A three-dimensional model for stage I-crack propagation

P. Köster, H. Knobbe, C.-P. Fritzen, H.-J. Christ, U. Krupp

The propagation of short fatigue cracks is simulated by means of a three-dimensional model. Under loading conditions in the high cycle fatigue regime the growth of these cracks can determine up to 90% of the lifetime of a component. Stage I-cracks often grow on slip bands and exhibit strong interactions with microstructural features such as grain boundaries. Experimental investigations have shown that the crack propagation rate decreases significantly when the crack tip approaches a grain boundary and even a complete stop of crack propagation is possible. In order to consider the real three-dimensional orientation of a slip plane an existing two-dimensional mechanism-based model (Künkler el al., 2008) is extended to simulate the propagation of a three-dimensional surface crack. The crack geometry is modelled using dislocation loops (Hills et al., 1996), which represent the relative displacement between the crack flanks. To describe the propagation of stage I-cracks elastic-plastic material behaviour is considered by allowing a plastic deformation due to slip on the active slip plane. The extension of the plastic zone is blocked by the grain boundary. The crack propagation law is based on the range of the crack tip slide displacement, which is obtained from the plastic solution. Behind the grain boundary the shear stress field is evaluated. Results show that a high twist angle between the slip planes causes a significant decrease in the stresses, which can yield a crack stop.

1 Introduction

Many components in industrial applications are subject to a cyclic loading in the high cycle fatigue regime. Under these conditions the fatigue process begins with the initiation of cracks, followed by short and long crack propagation until failure. In smooth components, the fatigue life is dominated by the stages of crack initiation and short crack propagation. Therefore, it is essential for a mechanism-based lifetime prediction model to describe the damage evolution in these stages correctly.

In polished test specimens, fatigue cracks often initiate trans- or intercrystalline at positions in the microstructure, which are subject to elevated stress. This stress increase can be caused by inclusions or the anisotropic elastic properties of the individual grains. After initiation, the following early crack growth occurs in stage I on individual, favourably orientated slip bands characterized by a high Schmid factor. The propagation rate is controlled by the cyclic plastic shear deformation at the crack tip. The growth of these short cracks in the microstructure of a duplex steel, as shown in Figure 1 has been studied by Krupp et al. (2004) and Düber et al. (2006).

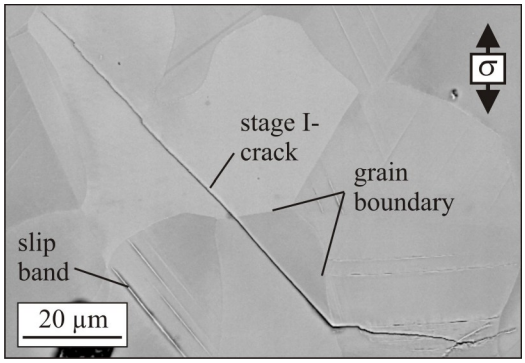

Figure 1. Stage I-crack in a duplex stainless steel

The grain boundaries act as microstructural obstacles to crack propagation, as they prevent a transmission of slip into the neighbouring grain. This yields a dislocation pile up in front of the barrier resulting in a decreased crack

growth rate. If the boundary is broken, the stress intensity will be relieved by slip in the next grain and the crack propagation rate will increase again. Thus, an oscillating crack growth is observed. The crack can grow through several grains in stage I. As the crack is deflected at grain boundaries, a zig-zag-shaped crack path is observed.

With increasing crack length additional slip systems are activated at the crack tip and the crack propagates on alternating slip systems. The crack path is deflected from a plane subject to maximum shear stress into a direction perpendicular to the applied load. The effect of the microstructure on the crack decreases more and more and finally the crack propagates in stage II under mode I.

As the propagation kinetics of short and long cracks are substantially different, it is not possible to simulate the whole fatigue process using one single model. The propagation of long cracks under mode I can be described either by elastic-plastic or linear elastic fracture mechanics. However, the special behaviour of short cracks requires models, which take microstructural effects into account. Approaches that fulfil this requirement are the analytical models of Taira et al. (1978) and Navarro and de los Rios (1988) where the crack propagation rate is predicted successfully using the crack tip slide displacement *CTSD*. The extension of the plastic zone is blocked by the next grain boundary until a critical stress in a dislocation source behind the barrier is reached to activate a new slip band. Based on this idea a two-dimensional model has been developed (Schick, 2004; Künkler, 2007; Künkler et al., 2008), which is able to predict crack growth in a real microstructure and considers the orientation of available slip systems in the crystals. The boundary value problem is solved numerically by means of a discretisation with dislocation dipole boundary elements.

According to Navarro and de los Rios, the fatigue limit of a material can be interpreted as the stress amplitude below which crack propagation stops at grain boundaries. In this case, the shear stress on a dislocation source behind the barrier is not high enough to activate slip. Therefore, it is essential for a model to predict the stress state behind a grain boundary correctly, which depends in addition to the external loading and the Schmid factor on the misorientation between the slip planes. This orientation relation can be expressed by a tilt and a twist angle. The former one, which is the angle between the slip traces on the surface, is already considered by the two-dimensional model. But according to Zhai et al. (2000) the barrier strength of a grain boundary is dominated by the twist angle between the slip planes so that the crack path is characterized by small twist angles between the slip planes. Furthermore, the crack depth also affects the stress state behind the grain boundary. In order to consider these effects the two-dimensional model of Künkler et al. (2008) is extended to a three-dimensional one for surface cracks in a semi-infinite body. The three-dimensional surface crack is modelled by a continuous distribution of dislocation loops (Hills et al., 1995). As the extension to three dimensions increases the complexity of the model significantly the work will be focused on the crack growth inside the first grain.

2 Modelling of stage I-crack growth

The existing two-dimensional stage I-model (Künkler et al., 2008) treats the crack and its plastic zone as yield strips and describes the growth of a stage I-crack on slip bands in a microstructure (Figure 2a). It allows an opening of the crack and a slide displacement between the crack flanks. Elastic plastic material behaviour is considered by permitting slip on the active slip band in front of the crack tip. Plastic deformation occurs if the shear stress τ on this slip band reaches the critical value for dislocation motion τ^b. The barrier effect of a grain boundary is considered by confining the extension of the plastic zone to the first grain. Only if a critical stress intensity on a dislocation source behind the grain boundary is reached, the respective slip plane is activated and slip is transferred into the next grain.

Analogous to the model of Navarro and de los Rios the crack propagation rate is calculated using a power law function based on the range of the crack tip slide displacement $\Delta CTSD$:

$$\frac{da}{dN} = C \cdot \Delta CTSD^m \tag{1}$$

Here, C is a material-specific constant and m is an exponent ($m \approx 1$). A physical explanation for the mechanism of crack propagation is given by the model of Wilkinson et al. (1998). During the loading and the unloading cycle dislocations of opposite sign are created in a dislocation source in front of the crack tip and move towards the crack. Thus, vacancies are generated, which lead to a crack advance.

The two-dimensional crack problem is solved numerically by means of a discretisation with dislocation dipole boundary elements, which represent a constant relative displacement over the element. The crack elements consist of two dislocation dipoles with a Burgers vector parallel and normal to the crack to allow for a slide and an opening displacement of the crack flanks. In the slip band only sliding is possible so the respective elements only consist of a dislocation dipole parallel to the crack. The elements are connected to each other by the influence function G^{ij}, which describes the stress in an element *i* due to a displacement in an element *j*. The total stress σ^i_{nn} and τ^i_{tn} is obtained by summation over all elements plus the external normal and shear stress $\sigma^{i\infty}_{nn}$ and $\tau^{i\infty}_{tn}$. The consideration of the boundary conditions yields the following system of inequalities:

$$\sigma^i_{nn} = \sum_{j=1}^{p} G^{ij}_{nn,n} b^j_n + \sum_{j=1}^{p+q} G^{ij}_{nn,t} b^j_t + \sigma^{i\infty}_{nn} \le 0 \qquad i = 1 \ldots p \tag{2}$$

$$\left|\tau^i_{tn}\right| = \left| \sum_{j=1}^{p} G^{ij}_{tn,n} b^j_n + \sum_{j=1}^{p+q} G^{ij}_{tn,t} b^j_t + \tau^{i\infty}_{tn} \right| \quad \begin{cases} = 0 & i = 1 \ldots p \\ \le \tau^b & i = p+1 \ldots p+q \end{cases} \tag{3}$$

$$b_n \ge 0 \qquad i = 1 \ldots p \tag{4}$$

Here, *p* is the number of crack elements and *q* the number of elements in the plastic zone. Inequality (4) states that the crack faces must not penetrate each other, hence, the model accounts for roughness-induced crack closure effects.

In this paper, the two-dimensional modelling approach is extended to three-dimensions so that the growth of surface cracks can be simulated (Figure 2b). Thus, an arbitrary shaped crack on a slip plane is considered and plastic deformation due to slip is possible on the entire slip plane in front of the crack front.

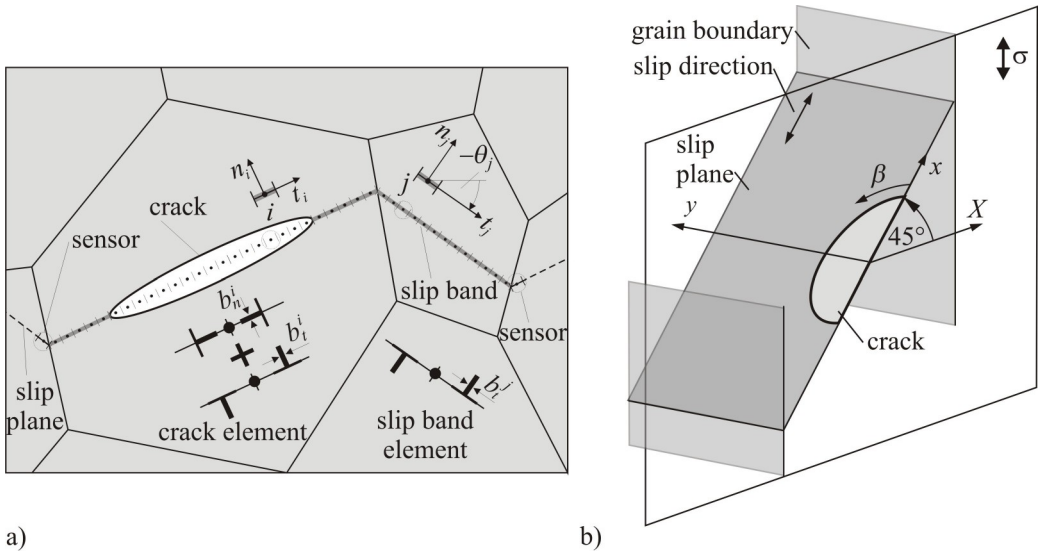

Figure 2. Two-dimensional stage I-crack model with boundary elements (a) and extension of the model to consider three-dimensional surface cracks

3 Extension of the model to three dimensions

In the three-dimensional case the dislocation dipole elements have to be replaced by dislocation loop elements to describe the relative displacement of the crack flanks. These elements have been developed by Dai et al. (1993) and Hills et al. (1996) and have been applied successfully to calculate the stress intensity factors of various three-dimensional crack shapes. In the following the main aspects of this approach will be presented.

3.1 Modelling of three-dimensional cracks

To derive the governing equations an arbitrary surface crack on a slip plane subject to the external loading σ_{jk}^{∞} is considered (Figure 3). Then, the relative displacement between the crack flanks can be modelled by a continuous distribution of infinitesimal loops *dS*. The stress field around such a dislocation loop of strength $b_m dS$ located at $\mathbf{x}'$ is known, so the total stress at a point **x** can be calculated by integration over the crack surface *S*. The distance between **x** and $\mathbf{x}'$ is $r^2 = r_i r_i$ and $r_i = x_i - x'_i$. By enforcing that the surface of an open crack is traction free the following integral equation is obtained:

$$\sigma_{jk}(\mathbf{x}) = \int_S K_{jkm}(\mathbf{x},\mathbf{x}')b_m(\mathbf{x}')dS + \sigma_{jk}^{\infty}(\mathbf{x}) = 0 \tag{5}$$

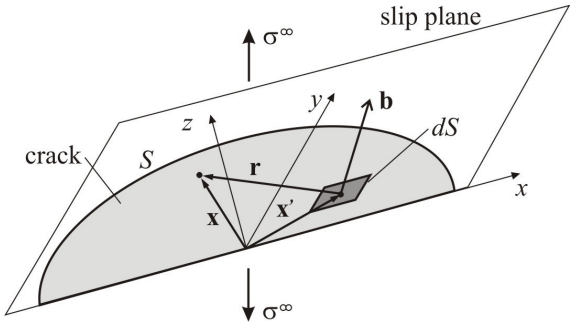

Figure 3. Three-dimensional surface crack

The kernel K_{jkm} is given in Dai et al. (1993) and can be split into two parts:

$$K_{jkm} = K_{jkm}^{s} + K_{jkm}^{c} \tag{6}$$

The first one K_{jkm}^{s} is the solution for an infinitesimal dislocation loop in an infinite solid and the second one K_{jkm}^{c} is a corrective term that accounts for the free surface of an infinite half space. The kernel K_{jkm}^{s} can be derived from the Green's function of an infinite body and reads:

$$K_{jkm}^{s}(\mathbf{x},\mathbf{x}') = -\frac{C_{ilm3}}{8\pi(1-\nu)}\frac{\partial}{\partial x'_l}\left[\frac{1}{r^2}\left(\frac{1-2\nu}{r}\left(\delta_{ij}r_k + \delta_{ki}r_j - \delta_{jk}r_i\right) + 3\frac{r_j r_k r_i}{r^3}\right)\right] \tag{7}$$

Here, C_{ilm3} are the elastic constants, ν is Poisson's ratio and δ_{ij} is the Kronecker delta. If the crack lies entirely in one plane, e.g. $z = 0$, all components depending on r_3 vanish and the complexity of the kernel reduces significantly. However, the complete kernel as given in (7) is required to calculate the shear stress on an arbitrary oriented slip plane behind the grain boundary. Explicit expressions for the corrective term K_{jkm}^{c}, which accounts for the presence of a free half space can be found in Hills et al. (1996).

As the kernel function (7) is hypersingular with a third order singularity when *r* approaches zero, the integral in (5) only exists in a finite parts sense. To solve this problem the semi-analytical method proposed by Hills et al. (1996) is used.

3.2 Numerical treatment

To solve the singular integral equation (5) numerically, the crack and the plastic zone are meshed with finite dislocation loop elements. Here, the linear non-conforming elements developed by Dai et al. (1996) are used that express the displacement field inside each element by a set of shape functions N_q:

$$b_m = N_q(\xi_1, \xi_2) b_m^q \qquad q = 1,...,n_c \tag{8}$$

Here, n_c is the number of collocation points lying inside of the element, b_m^q is the displacement discontinuity at these collocation points and ξ_1, ξ_2 are the local element coordinates. It is possible to use both triangular and quadrilateral elements where a point inside the element is defined as:

$$x_j = L_p(\xi_1, \xi_2) x_j^p \qquad p = 1,...,n_d \tag{9}$$

The number of nodes is n_d, x_j^p are the nodal coordinates and L_p are the standard shape functions for linear elements. By substituting the approximation for b_m (8) into the integral (5) the following system of linear equations is obtained, which relates the unknown relative displacement of the crack flanks to the external loading:

$$K_{jkm}^{st} b_m^t = -\sigma_{jk}^{\infty}\left(x^s\right) \qquad s,t = 1,...,n_t\,. \tag{10}$$

Here, n_t is the total number of collocation points and K_{jkm}^{st} is given by:

$$K_{jkm}^{st} = \int_{S_n} K_{jkm}\left(\mathbf{x}^s, \mathbf{x}(\xi_1, \xi_2)\right) N_q(\xi_1, \xi_2) \left|J(\xi_1, \xi_2)\right| d\xi_1 d\xi_2 \tag{11}$$

$\left|J(\xi_1, \xi_2)\right|$ is the determinant of the Jacobian and the domain of integration S_n is the area of element n. If the point x^s is outside of S_n, the integral is regular and can be calculated by standard Gaussian quadratures. Otherwise the semi-analytical method mentioned above will be applied.

4 Applications of the model

First, the previously presented model is applied to study the effect of crack depth on the stress field behind the grain boundary. Therefore, a rectangular crack on a slip plane (Figure 4) is considered. The crack length is $2a = 100\mu m$ and the crack depth c is increased from 20 µm to 100 µm (Figure 5a). In all simulations, the external loading is 400 MPa. The shear stress field behind the grain boundary is measured by sensors positioned on a circle around the crack front. Results are given with respect to the slip band angle θ between the direction of the sensor and the horizontal axis. The values are compared to those of the two-dimensional model, which represents a crack with infinite depth in a plate.

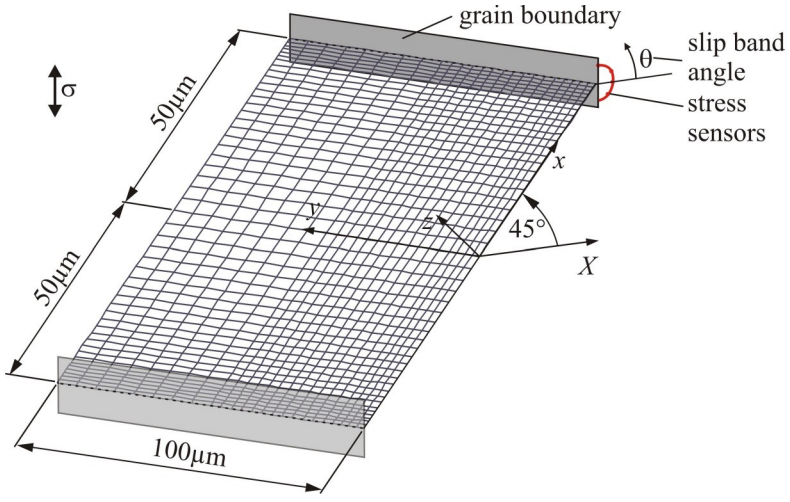

Figure 4. Mesh for a rectangular crack on a slip plane

The shear stress increases significantly with increasing crack depth (Figure 5b). Comparing the results to those obtained by the two-dimensional model, a good correlation in the shape of the stress field can be found. Furthermore, the shear stress seems to converge to the two-dimensional solution as the values for an aspect ratio $c/a = 2$ are only slightly below those of a through thickness crack in a plate.

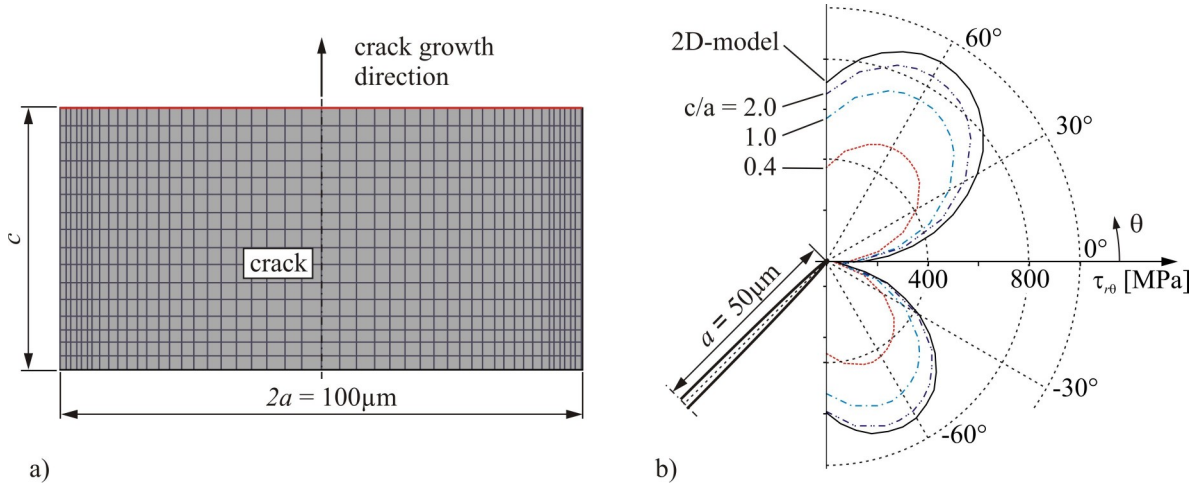

Figure 5. Crack propagating into the interior (a) and effect of crack depth on shear stress field behind the grain boundary (b)

By means of polishing experiments on fatigue test specimens Wagner (1989) found that stage I-cracks grow fast at the surface until they reach the next grain boundary. Then crack propagation stops at the surface and the crack only grows into the interior. Finally, after arresting in front of the grain boundary for a number of cycles, the crack overcomes the barrier at the surface and continues to grow into the next grain. The three-dimensional model presented here can be used to explain this effect. If the crack is still shallow, the shear stress in front of the crack tip is not sufficient to activate slip systems in the neighbouring grain behind the grain boundary. However, as the stress increases with increasing crack depth, the critical value for activating a dislocation source is finally reached.

Furthermore, the propagation of a rectangular crack of constant depth towards the grain boundary is simulated, where the crack length $2a$ is increased by one row of elements each cycle, starting with an initial crack length of $a = 20\mu m$. Once more the mesh shown in Figure 4 is used. Now, a plastic zone is considered between the crack front and the grain boundary, where plastic deformation due to slip is possible. The microstructural shear strength is $\tau^b = 99MPa$. This value has been measured by means of Hall-Petch experiments on a ferritic steel (Düber et al., 2006). In order to be able to compare the results to the two-dimensional model the slip direction is assumed to be parallel to the surface.

In Figure 6a the maximum plastic deformation at the crack front and the free surface is plotted over the crack length for various crack depths. As an irreversible plastic deformation at the crack front is considered to be responsible for crack growth, the results are proportional to the crack propagation rate (1). Due to the rather low shear strength on a slip plane, high values for the plastic deformation at the crack tip are calculated even for short cracks. However, while the distance between crack front and grain boundary decreases, *CTSD* reduces as well. Once again, a significant effect of crack depth is observed. The results for a deep crack with $c = 100\mu m$ are about twice as high as those for a shallow crack with $c = 20\mu m$ and only slightly below the values calculated by the two-dimensional model.

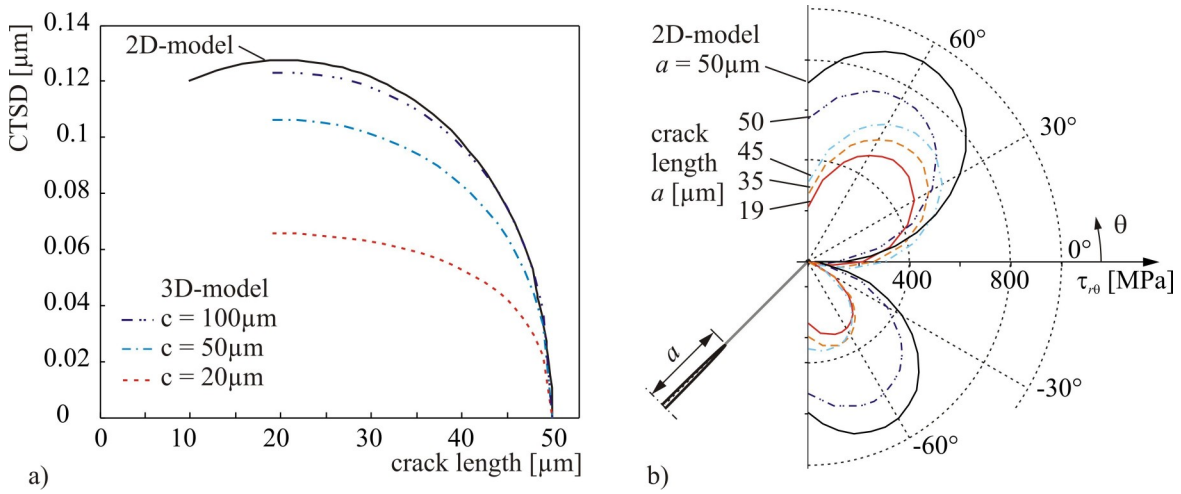

Figure 6. Crack tip slide displacement (a) and the evolution of the shear stress field behind the grain boundary with increasing crack length, crack depth $c = 50\mu m$ (b)

Finally, the developed three-dimensional short crack model is used to simulate the growth of a semi-circular surface crack on a slip plane (Figure 2b). The initial crack length is $a = c = 10\mu m$ and the slip plane is assumed to be rectangular with a surface length of 100 µm and a depth of 50 µm. The geometry is meshed using 1062 quadrilateral elements (Figure 7a) and a cyclic loading of $\sigma = \pm 400 MPa$ is applied. In order to obtain accurate results at the crack front, the mesh is refined in this region.

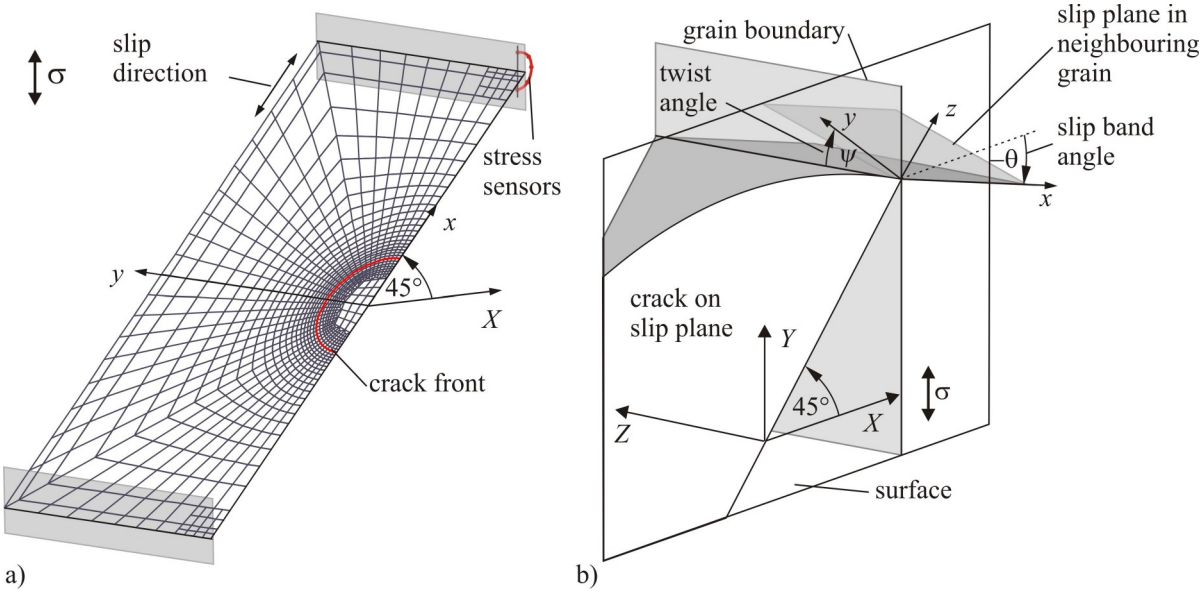

Figure 7. Mesh of semi-circular surface crack on slip plane (a) and orientation of possible slip plane behind the grain boundary (b)

First, convergence has been tested by comparing the results of *CTSD* along the crack front for different meshes between 738 elements and 1206 elements. The error compared to the finest mesh decreases with an increasing number of elements and is always below 1 % (Figure 8). The relative error for the mesh, which is used for the crack growth simulation, is even below 0.3 %.

In order to simulate the growth of the starter crack on the slip plane the crack propagation law (1) based on the irreversible plastic deformation at the crack front is implemented in the model. At this stage, it is possible to differentiate between the loading conditions along the crack front, changing from mode I+II at the surface to mode I+III at the deepest point of the crack. Pokluda et al. (2008) suggest a reduced crack propagation rate under mode III as no free surface is generated in this mode. However, as an explicit factor for the difference between mode II and III is not given, no differentiation between mode II and III is made here.

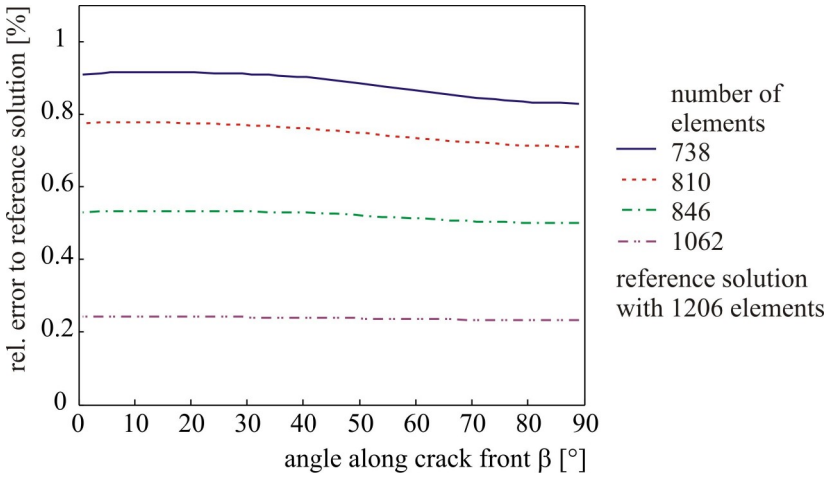

Figure 8. Relative error in *CTSD* compared to finest mesh

In the simulation the crack extension is calculated after each load cycle. Then the mesh is updated to the new crack geometry and the new influence functions K^{st}_{jkm} are calculated. This procedure is repeated until the crack reaches the grain boundary and the simulation is stopped, in this case after 54 load cycles. When the distance between crack and the grain boundary gets too small the plastic zone cannot be meshed anymore using well shaped quadrilateral elements. In this case triangular elements are used.

During the crack growth simulation, the shear stress field behind the grain boundary is calculated (Figure 9a). For a short crack high shear stresses are found in the extension of the slip plane. This can be explained by the low shear strength, which causes plastic deformation on the whole slip plane resulting in a mode II stress singularity behind the grain boundary. With increasing crack length, the shear stress increases on possible slip systems. Finally, when the crack front has reached the grain boundary, the effect of the opening mode I yields a change in the stress field, especially in the lower half of Figure 9a.

So far, only a tilt angle between the crack plane and a possible slip plane in the neighbouring grain is considered. However, an additional twist angle is also possible as shown in Figure 7b. To calculate the effect of this twist on the shear stress field, the stress tensor is transformed. For the crack in front of the grain boundary the results are plotted in Figure 9b for various twist angles over the slip band angle. With increasing twist angle the shear stress reduces significantly. Thus, it gets more and more unlikely that a dislocation source is activated behind the grain boundary.

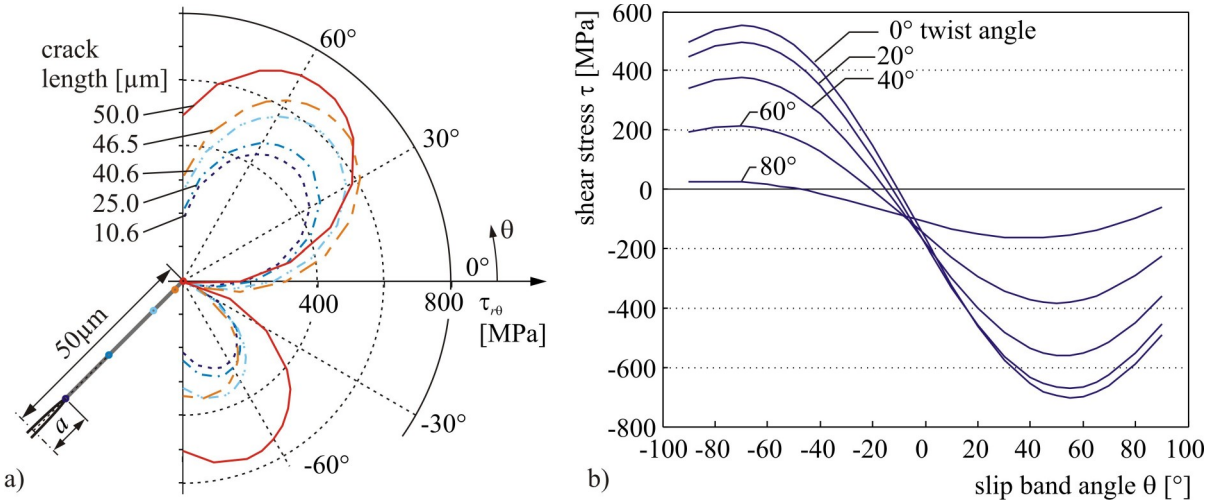

Figure 9. Evolution of shear stress field behind the grain boundary (a) reduction of shear stress with increasing twist angle (b)

5 Conclusions

A two-dimensional model (Künkler et al., 2008), which is able to predict the abnormal propagation of microstructurally short stage I-cracks, is extended to three dimensions. The model considers elastic plastic material behaviour by allowing slip on the active slip plane. The crack problem is solved numerically using finite dislocation loop elements so only the crack and the plastic zone have to be meshed. To consider the barrier effect of grain boundaries on plastic deformation and crack growth, the extension of the plastic zone is limited to the first grain. The shear stress acting on a dislocation source behind the grain boundary is considered as a criterion for the transmission of slip into the neighbouring grain. While the two-dimensional model only considers the tilt angle between the slip planes directly, it is now possible to study the effect of an additional twist angle as well as the crack depth on the shear stress field.

First, the new model is compared to the existing two-dimensional one by using a rectangular crack. It is found that the shear stress increases significantly with increasing crack depth. For a deep crack with an aspect ratio $2a/c = 1$ the result is only slightly below the two-dimensional solution of a crack in an infinite plate. Furthermore, a crack propagation law based on the plastic shear deformation at the crack front is implemented in the model and the growth of an initial semi-circular surface crack is simulated. During crack growth the shear stress on possible slip systems behind the grain boundary is monitored. The results show that an additional twist angle yields a significant decrease of the shear stress. So it becomes more and more unlikely that slip is activated on a highly twisted slip plane.

As the three-dimensional modelling is much more complex than the two-dimensional case, crack propagation is so far limited to the first grain. Nevertheless, work will be continued to consider crack growth over the grain boundary, leading to a crack deflection and geometrically induced crack closure.

References

Dai, D. N.; Nowell, D.; Hills, D. A.: Eigenstrain methods in three-dimensional crack problems: an alternative integration procedure. *J. Mech. Phys. Solids*, 41 (1993), 1003-1017.

Dai, D. N.; Hills, D. A.; Nowell, D.: Formulation and implementation of the eigenstrain method employing higher order elements. *Int. J. Solids Structures*, 33, (1996), 331-342.

Düber, O.; Künkler, B.; Krupp, U.; Christ, H.-J.; Fritzen, C.-P.: Experimental characterization and two-dimensional simulation of short-crack propagation in an austenitic–ferritic duplex steel. *Int. J. Fatigue*, 28, (2006), 983-992.

Hills, D. A.; Kelly, P. A.; Dai, D. N.; Korsunsky, A. M.: *Solution of crack problems*. Kluwer Academic Publishers, London (1996).

Krupp U, Düber O, Christ H.-J., Künkler B, Schick A, Fritzen C.-P.: Application of the EBSD technique to describe the initiation and growth behaviour of microstructurally short fatigue cracks in a duplex steel. *J. of Microscopy*, 213, (2004), 313-320.

Künkler, B.: *Mechanismenorientierte Lebensdauervorhersage unter Berücksichtigung der Mikrostruktur.* VDI-Verlag, Düsseldorf (2007).

Künkler, B.; Düber, O.; Köster, P.; Krupp, U.; Fritzen, C.-P.; Christ, H.-J.: Modelling of short crack propagation – Transition from stage I to stage II. *Engng. Fract. Mech.*, 75, (2008), 715-725.

Navarro, A.; de los Rios, E. R.: Short and Long Fatigue Crack Growth: A Unified Model. *Phil. Mag. A*, 57, (1988), 15-36.

Pokluda, J.; Trattnig, G.; Martinschitz, C.; Pippan, R.: Straightforward comparison of fatigue crack growth under mode II and III. *Int. J. Fatigue*, 30, (2008), 1498-1506.

Schick, A.: *Ein neues Modell zur mechanismenorientierten Simulation der mikrostrukturbestimmten Kurzrissausbreitung*. VDI-Verlag, Düsseldorf (2004).

Taira, S.; Tanaka, K.; Nakai, Y.: A Model of Crack-Tip Slip Band Blocked by Grain Boundary. *Mechanics Research Communications*, 5, (1978), 375-381.

Wagner, L.: *Mikrorissausbreitung in hochfesten Titan- und Aluminiumlegierungen*. Habilitationsschrift, Universität Hamburg-Harburg (1989).

Wilkinson, A. J.; Roberts, S. G.; Hirsch, P. B.: Modelling the threshold conditions for propagation of stage I fatigue cracks. *Acta Mater.*, 46, (1998), 379-390.

Zhai, T.; Wilkinson, A. J.; Martin, J. W.: A crystallographic mechanism for fatigue crack propagation through grain boundaries. *Acta Mater.*, 48, (2000), 4917-4927.

Address: Philipp Köster and Prof. Dr.-Ing. Claus-Peter Fritzen, Institut für Mechanik und Regelungstechnik, Helge Knobbe und Prof. Dr.-Ing. Hans-Jürgen Christ, Institut für Werkstofftechnik, Universität Siegen, D-57068 Siegen, Prof. Dr.-Ing. Ulrich Krupp, Fakultät Ingenieurwissenschaften und Informatik, Fachhochschule Osnabrück, 49076 Osnabrück.
email: koester@imr.mb.uni-siegen.de